

Towards the absolute planes: a new calibration of the Bolometric Corrections and Temperature scales for Population II Giants [★]

P. Montegriffo,¹ F.R. Ferraro,¹ L. Origlia,¹ and F. Fusi Pecci^{2†}

¹*Osservatorio Astronomico di Bologna, Via Zamboni 33, 40126 Bologna, ITALY*

²*Stazione Astronomica, 09012 Capoterra, Cagliari, ITALY*

31 May 2021

ABSTRACT

We present new determinations of bolometric corrections and effective temperature scales as a function of infrared and optical colors, using a large database of photometric observations of about 6500 Population II giants in Galactic Globular Clusters (GGCs), covering a wide range in metallicity ($-2.0 < [\text{Fe}/\text{H}] < 0.0$).

New relations for BC_K vs (V-K), (J-K) and BC_V vs (B-V), (V-I), (V-J), and new calibrations for T_{eff} , using both an empirical relation and model atmospheres, are provided.

Moreover, an empirical relation to derive the R parameter of the Infrared Flux Method as a function of the stellar temperature is also presented.

Key words: Clusters: Globular – Stars: Evolution – Stars: Fundamental Parameters – Stars: Hertzsprung–Russell diagram – Photometry: IR–Array

1 INTRODUCTION

A global test of stellar evolutionary models requires a direct comparison between theoretical tracks and observations for stars spanning a wide range in stellar parameters, such as temperature, luminosity and metallicity. In order to achieve these goals at least two fundamental ingredients are needed:

- i)* a complete and homogeneous database of photometric observations;
- ii)* a suitable set of transformations between observables and absolute quantities.

GGCs are the best empirical laboratory to obtain complete and homogeneous spectrophotometric information on Pop. II stars over a wide range of metallicities.

Reviewing the published works on the transformations to the absolute plane (see Sect.3), that is bolometric corrections (BCs) and temperature scales as a function of different colors, it is easy to see that very often these calibrations are not based on a complete and homogeneous set of data, spanning a wide range of stellar parameters. Moreover, *ad hoc* correction factors are usually adopted to take into account for example possible systematic differences between different photometric systems and/or different assumptions

for the reference solar quantities, for the adopted model atmospheres, and for different laws to extrapolate the data towards the UV/IR ranges.

Such a scenario indicates that any calibration in the absolute plane can hardly be fully self-consistent as it always depends on the adopted transformations and, more crucial, the residuals among different scales are very rarely linear with the involved parameters.

In order to improve the available determinations of the bolometric corrections and temperature scales, we use here our IR photometric database on GGC stars combined with available optical data from the literature to calibrate new, independent, (hopefully) self-consistent transformations, particularly useful to study the red stellar sequences in Pop II stars.

In Sect.2 we present the complete database used in our analysis which includes about 6500 RGB and HB stars in a sample of 10 GGCs observed in both optical and near IR bands. In Sect.3 we derive the transformations from observed magnitudes and colors to absolute quantities, such as bolometric corrections and effective temperatures. All the results are listed in Table 3. In Sect.4 we compare the inferred scales with existent ones and we give a fully empirical calibration of the R parameter of the Infrared Flux Method (IRFM) as a function of the effective temperature. Schematic conclusions are eventually presented in Sect.5.

[★] Based on data taken at the ESO–MPI 2.2m Telescope equipped with the near IR camera IRAC2 - ESO, La Silla (Chile).

[†] on leave from Osservatorio Astronomico di Bologna

2 THE DATABASE

The IR database used in this study includes photometric observations in J and K bands of about 17000 stars belonging to 10 GGCs spanning the whole range in metallicity (from $[\text{Fe}/\text{H}] = -2.15$ to $[\text{Fe}/\text{H}] \approx 0.0$). The data were obtained at ESO, La Silla (Chile), during two different runs (on June 1992 and June 1993), using the ESO-MPI 2.2m telescope and the near-IR camera IRAC-2 (Moorwood et al. 1992) equipped with a NICMOS-3 256x256 array detector. The complete description of the observations and data reduction can be found in Ferraro et al. (1994a,b) and Montegriffo et al. (1995) and in a series of forthcoming papers, where each individual cluster is discussed in more detail.

Our IR database was cross-correlated with other optical and IR catalogs in the literature in order to provide complete UBVRIJK photometry of as many stars as possible. The final sample used in the following analysis includes about 6500 RGB and HB stars.

The reddening correction in each photometric band was performed starting from the $E(B-V)$ color excess (as reported by Armandroff (1989) with the exception of M68 and M69 for which we used the values by Walker 1994 and Ferraro et al. 1994a, respectively) and using the extinction law proposed by Rieke & Lebovsky (1985). In Table 1 the main features of the database are listed: the GGC names, the cluster metallicity as quoted by Zinn (1985), the available photometric bands, and the adopted $E(B-V)$ color excess. In the following the observed colors are always corrected for reddening.

2.1 Notes on individual clusters

M15: UBVR photometry from Stetson (1994).

M30: UBV photometry from Bergbusch (1996).

M68: BVI photometry from Walker (1994).

M55: BV photometry from Piotto (1996) and VI from Ortolani & Desidera (1996): V was averaged.

M4: BV photometry from Lee (1977).

M107: BV photometry from Ferraro et al. (1991).

M69: BV photometry from Ferraro et al. (1994a).

47Tuc: UBV photometry from Auriere & Lauzeral (1996) and VI from Ortolani & Desidera (1996). The VI photometry was compared with that one obtained by Da Costa & Armandroff (1990) for the few stars in common. There is an excellent agreement in V, while a systematic shift in the zero point by about 0.12 mag in I has been found: we applied this correction to the I photometry from Ortolani & Desidera (1996).

NGC6553: VI photometry from Guarnieri et al. (1997) using HST data.

NGC6528: VI photometry from Ortolani et al. (1995) using HST data.

3 ABSOLUTE QUANTITIES

Various calibrations of the bolometric correction and temperature scale have been proposed by different authors since many years.

Table 1. Adopted IR and optical database.

Cluster		[Fe/H] ^a	Photometry ^b	$E(B-V)$ ^c
NGC7078	M15	-2.15	UBVRJK	0.10
NGC7099	M30	-2.13	UBVJK	0.04
NGC4590	M68	-2.09	BVIJK	0.07
NGC6809	M55	-1.82	BVIJK	0.06
NGC6121	M4	-1.19	BVJK	0.40
NGC6171	M107	-0.89	BVJK	0.31
NGC6637	M69	-0.75	BVJK	0.17
NGC104	47Tuc	-0.70	UBVIJK	0.04
NGC6553		-0.29	VIJK	0.78
NGC6528		-0.07	VIJK	0.56

^a From Zinn (1985).

^b J,K from our IR-array survey, U,B,V,R,I from the literature (refers to Sect.2.1 for the bibliographic sources).

^c $E(B-V)$ from Armandroff (1989), but M68 from Walker (1994) and M69 from Ferraro et al. (1994a), respectively.

Johnson (1966) used a sample of 15 giants observed in the UBVRIJKLMN to get bolometric corrections in the V band, integrating the spectral energy distribution and applying small corrections (<0.1 mag) in the wavelength ranges not covered by his survey (such as for example the H band) to take into account possible molecular blending in cool stars. The zero point is defined as $BC_V^\odot = 0.00$.

Carney & Aaronson (1979) reconstructed the energy distribution of a sample of dwarfs and subdwarfs by means of polynomial fits to the optical photometry, while the UV range was extrapolated using the Kurucz (1979) models and the IR region using blackbodies. Their zero point is $BC_V^\odot = -0.12$.

Frogel, Persson & Cohen (1981, hereafter FPC81) performed trapezoidal integrations of the energy distribution of a sample of stars observed in the UBVRIJHKL, and extrapolating the UV and IR fluxes. They adopted as zero point the value $BC_V^\odot = -0.08$.

More recently, Tinney et al. (1993) reconstructed the spectral energy distribution of cool stars combining photometric data in the VIJHKLL' bands with low resolution spectra.

Alonso et al. (1995) determined the bolometric corrections in the K band of a sample of F,G,K dwarfs. They performed trapezoidal integrations using UBVRIJHK photometric data and included a correction factor $C = f(T_{\text{eff}}, \log g, [\text{Fe}/\text{H}])$ to the UV and IR fluxes as a function of the stellar parameters, using the Kurucz (1993) models.

Concerning the determination of the stellar effective temperature, the only pure experimental way to derive it is to know the star intrinsic luminosity and apparent angular diameter. Ridgway et al. (1979) for example measured the angular diameter of a sample of nearby Pop I giants by means of lunar occultations, while Di Benedetto & Rabbia (1987, hereafter DBR87) and Di Benedetto (1993, hereafter DB93) used interferometric techniques.

Once the apparent stellar diameters have been measured, the effective stellar temperatures can be estimated assuming a proper scale of bolometric corrections. DBR87 have shown how an error of 0.05 mag in the determination of the BC_K transfers into an error of ≈ 60 K in the temperature estimates for T_{eff} around 5000 K and of ≈ 35 K for $T_{\text{eff}} \approx 3000$ K. These uncertainties are of the same or-

Table 2. Absolute flux calibrations of a zero magnitude star in UBVRIJHKL bands for different photometric systems. Wavelengths are in μm and fluxes in units of $10^{-8} \text{ erg s}^{-1} \text{ cm}^{-2} \mu\text{m}^{-1}$.

Filter	Johnson ^a		Bessell ^b		ESO ^c	
	λ_{eff}	f_{λ_0}	λ_{eff}	f_{λ_0}	λ_{eff}	f_{λ_0}
U	0.36	4345	0.366	4175	0.363	4080
B	0.44	7194	0.438	6320	0.438	6490
V	0.55	3917	0.545	3631	0.548	3650
R	0.70	1762	0.641	2177	0.641	2190
I	0.90	829.9	0.798	1126	0.795	1180
J	1.25	289.7	1.221	314.7	1.244	312
H	1.62	107.9	1.632	113.8	1.634	120
K	2.20	38.02	2.187	39.61	2.190	41.7
L	3.50	7.834	3.451	7.080	3.770	5.41

^a Johnson system revised by Buzzoni (1996).

^b Bessell system adopted in BCP97 (Castelli 1997).

^c UBVRI from Bessell (1990) and from Megessier (1995).

der of magnitude as the empirical errors, hence an accurate estimate of BC_K is an important issue and severely affects the overall accuracy of the temperature estimated using this technique.

Another method which allows one to derive stellar temperatures in more distant objects is represented by the so-called IRFM proposed by Blackwell, Shallis & Selby (1979) and Blackwell & Lynas-Gray (1994).

This method uses as a fundamental parameter the quantity $R = f_{bol}/f_{\lambda}$, where f_{bol} is the observed bolometric flux and f_{λ} is the observed flux in a certain photometric band. Such a quantity is compared with the corresponding theoretical one, derived by means of models of atmospheres, in order to derive a temperature scale. Tinney et al. (1993) for their sample of dwarfs (see above) derived T_{eff} by subsequent iterations of the IRFM.

Finally, a fully theoretical approach is the extensive use of model atmospheres to derive synthetic colors for different input stellar parameters.

Before describing the adopted procedures to calibrate our relations, we want to add a further comment on a crucial point: each absolute flux calibration requires a reference zero-magnitude star in all the explored photometric bands, that is in the specific photometric system used. As pointed out by many authors (see e.g. Bessell & Brett 1988; Buzzoni 1989; Bessell 1990, Megessier 1995) the photometric CCD+filter characterization is often provided with a quite large uncertainty (typically $\approx 5\%$), and this may severely affect the accuracy of the derived quantities, particularly the bolometric fluxes, based on this instrumental calibration. Moreover, it is difficult to reconstruct the adopted values from the various authors since very often they are not tabulated. Since in the calibrations of the present paper we worked with different photometric systems, in Table 2 we report all the adopted zero magnitude fluxes.

3.1 The determination of bolometric corrections

3.1.1 The BC_K vs $(V-K)$ and $(J-K)$

For all the observed stars in the selected sample of GGCs we computed the bolometric correction BC_K in the K band

by means of the relation:

$$BC_K = m_{bol} - K$$

where m_{bol} is the apparent bolometric magnitude.

m_{bol} was computed as follows: first we convert the apparent magnitudes corrected for reddening into fluxes using the classical formula:

$$f_{\lambda} = f_{\lambda_0} \cdot 10^{-0.4 \cdot m_{\lambda}}$$

where f_{λ_0} is the absolute flux in a certain photometric band corresponding to the zero magnitude. We used the UBVJK filters of Johnson and RI of Cousins in the ESO standard photometric system. In Table 2 we report the absolute flux calibrations of a zero magnitude star for all the observed photometric bands, for different photometric systems. The values we adopted in our analysis are those listed in columns #6 and #7.

The energy distribution was reconstructed starting from a set of Planck functions $B_{\lambda}(T_c)$ computed between two adjacent observed bands, where T_c is the corresponding color temperature. We want to stress that the color temperature is here simply a "working parameter" and it is not used to constrain the effective stellar temperature.

The final dense grid was obtained interpolating between two adjacent bands and extrapolating in the UV and IR ranges not covered by the observations. The apparent bolometric magnitude was then computed by means of integration over the energy distribution as follows:

$$m_{bol} = -2.5 \log_{10} \int f_{\lambda} d\lambda + ZP$$

The zero point (ZP) of the bolometric scale is given by

$$ZP = M_{bol}^{\odot} + 2.5 \log_{10} (F_{bol}^{\odot})$$

so its actual value depends upon the assumed M_{bol}^{\odot} and F_{bol}^{\odot} . We used $M_{bol}^{\odot} = 4.75$, $M_V^{\odot} = 4.82$ (so $BC_V^{\odot} = -0.07$), $L_{bol}^{\odot} = 3.86 \times 10^{33} \text{ erg s}^{-1}$, as reported by Armandroff (1989), and the relation: $F_{bol}^{\odot} = L_{bol}^{\odot}/(4\pi d^2)$, where $d = 10 \text{ pc}$. We obtained $ZP = -11.478$.

The accuracy of the inferred bolometric magnitudes primarily depends on the number of observed bands since extrapolations over a wide wavelength range may represent a severe approximation of the true energy distribution.

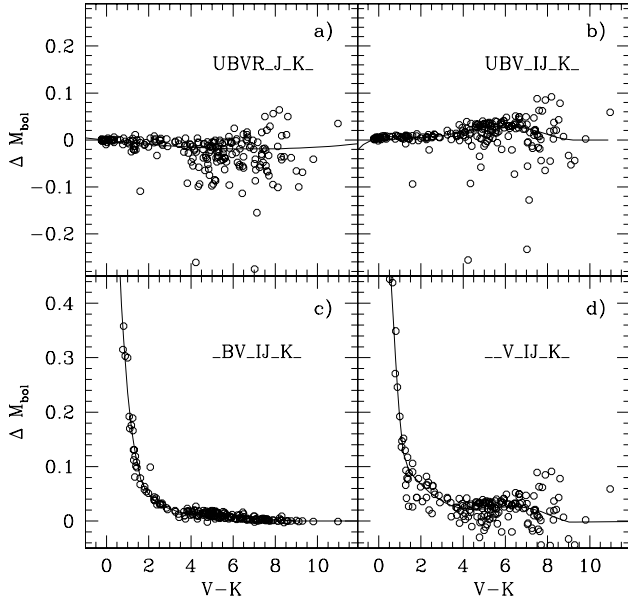


Figure 1. (a) m_{bol} (tot) – m_{bol} (UBVRJK), (b) m_{bol} (tot) – m_{bol} (UBVIJK), (c) m_{bol} (tot) – m_{bol} (BVIJK), and (d) m_{bol} (tot) – m_{bol} (VIJK) vs the (V-K) color (see Sect.3.1.1). m_{bol} (tot) was computed using the complete UBVRIJHKLMN set of filters. Open circles mark the stars by Morel & Magnenat (1978), while the continuous lines are our best fits.

In order to check the possible corrections to apply to the inferred values when a small number of bands was observed, we performed the following experiment: we used the catalog by Morel & Magnenat (1978) which contains 212 stars with a complete set of UBVRIJHKL photometry in the Johnson system and we applied our method to derive the apparent bolometric magnitudes with varying the number of available photometric bands, using the Johnson absolute flux calibration (columns #2 and #3 in Table 2).

In Fig.1 we plot as an example a few simulations of the differences between m_{bol} computed using all the Morel & Magnenat (1978) bands and only those available in our GGC database vs the (V-K) color. Similar simulations were performed using (J-K). The continuous line in the plots is our *numerical* best fit and represents the final corrections we applied to the bolometric magnitudes of the stars in our database as a function of their (V-K) and (J-K) colors and the available photometric bands.

On average, the discrepancies between the bolometric corrections computed using the entire set of photometric data and those computed using only a few bands are always within a few hundredths of a magnitude as one can see in Fig.1. Larger discrepancies, up to 0.1 mag, were found in the case of hot stars which lack U band observations: in this case, the UV continuum computed with a Planck function using the (B-V) color temperature is overestimated.

As a further check on the accuracy of the proposed method to derive the bolometric corrections we also reconstructed the energy distribution using direct trapezoidal integrations as suggested by many authors. The results of such a computation indicated that the corrections to apply if only

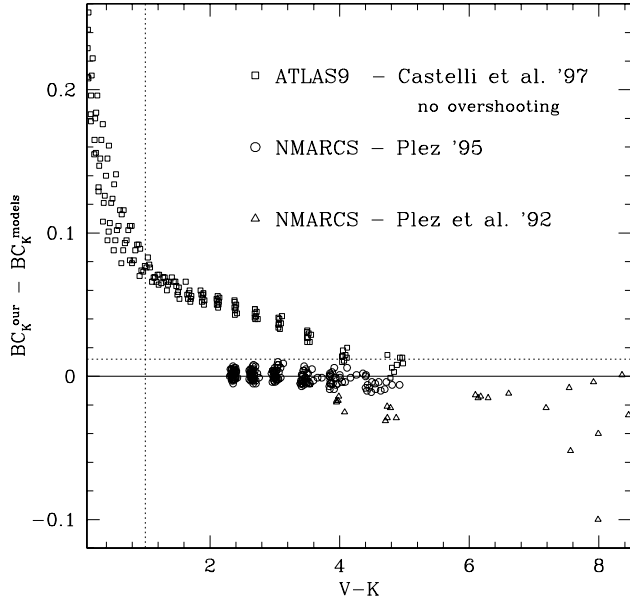


Figure 2. Differences between the inferred BC_K using our procedure and that of the models, as a function of the (V-K) color. This comparison is performed using as reference database the set of synthetic grids of stellar atmospheres by BCP97. The dashed horizontal line is a systematic zero point shift of ~ 0.01 between the two calibrations (our – models) (see Sect.3.1.1). At $(V-K) \leq 1$ the Balmer discontinuity strongly affects the accuracy of our BC_K .

a few colors are available should be even larger than in the case of integrations by means of Planck functions.

We did not apply any further correction due to the Balmer discontinuity in the UV and possible molecular sources of opacity in the IR. Nevertheless, we performed some tests to evaluate the entity of such an effect using UBVRIJHKL synthetic color indices computed by Bessell, Castelli & Plez (1997, hereafter BCP97) and derived from different grids of model atmospheres, which include both the ATLAS9 models computed without any overshooting for the convection (Castelli et al. 1997) and NMARCS models computed by Plez, Brett, & Nordlund (1992) and Plez (1995). The synthetic indices derived from Plez (1995) models are computed for T_{eff} ranging from 3600 K to 4750 K, gravity $\log g$ ranging from -0.5 to 3.5, and metallicities $[Fe/H] = -0.6, -0.3, 0.0, 0.3, 0.6$. Synthetic indices from ATLAS9 models and from Plez et al. (1992) models are tabulated only for the solar metallicity.

We computed the BC_K of these *synthetic* stars following the same procedure as for *true* stars in our database using the Bessell absolute flux calibration (columns #4 and #5 in Table 2). We compared the inferred values with those of the models themselves. The results of this comparison are plotted in Fig.2 as a function of the (V-K) color. For $(V-K) > 1$, the agreement between the two scales is satisfactory apart from an average shift in the zero point $\Delta BC_K = 0.01$, possibly ascribed to the different assumption on M_{bol}^\odot (they adopt $M_{bol}^\odot = 4.74$).

For bluer colors the agreement between the two scales gets exponentially worse and worse since the continuum

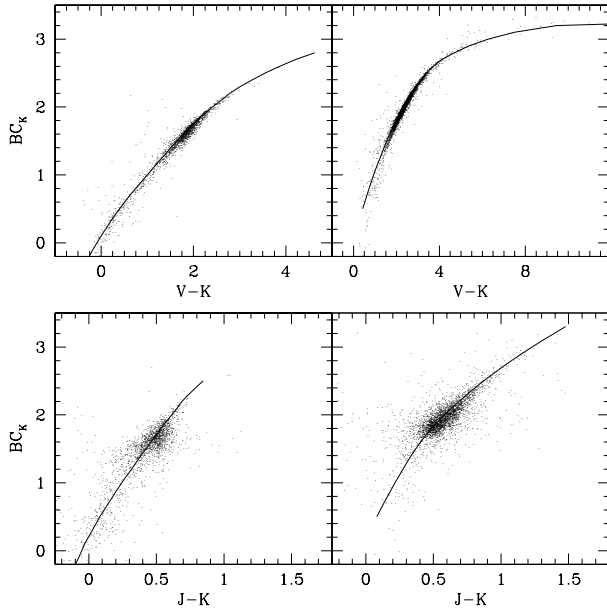


Figure 3. BC_K as a function of $(V-K)$ and $(J-K)$ colors for metal poor (left panels) and metal rich (right panels) stars. Continuous lines are our best fit.

shape is strongly affected by the Balmer discontinuity and a Planck function is unable to properly reproduce it.

In order to investigate a possible dependence of the bolometric correction *vs* color relations on the metallicity, we divided the observed clusters into two groups: one at low metallicity ($[Fe/H] < -1.0$), using about 2000 stars in M15, M30, M68, M55 and M4, and the other at higher metallicity ($[Fe/H] > -1.0$), using about 4500 stars in M107, M69, 47 Tuc, NGC6553 and NGC6528). We found a small (a few hundredths of a magnitude) difference when fitting our metal poor and metal rich stars in the empirical BC_K *vs* $(V-K)$ and $(J-K)$ planes, more evident at $(V-K) < 2$ and $(J-K) < 0.7$. This difference, that we want to stress is purely observational, could be explained in terms of a small metallicity dependence of the $(V-K)$ and $(J-K)$ colors as suggested by the model atmospheres whose continuum opacities, particularly at optical wavelengths, are slightly affected by changing the metal content. A similar behaviour was found by Alonso et al. (1995) using an independent, semi-empirical approach to estimate the bolometric flux (see Sect.1).

Nevertheless, since the difference we found is similar in size to the intrinsic photometric error, we cannot completely exclude the possibility that the observed effect is due to a systematic bias in the data.

In Fig.3, we plot the derived BC_K as a function of the $(V-K)$ and $(J-K)$ colors for metal poor and metal rich stars separately. Our best fits are shown as continuous lines. The relation with the lowest spread is, as expected, that based on the $(V-K)$ color which has the largest wavelength baseline.

In Table 3 we report the corresponding BC_K values as a function of the $(V-K)$ and $(J-K)$ colors from our best fits, both for metal poor and metal rich stars. The BC_K is fixed (in other words we fixed the stellar temperature, see next section) and the colors slightly change (≤ 0.1 mag) in the two metallicity regimes.

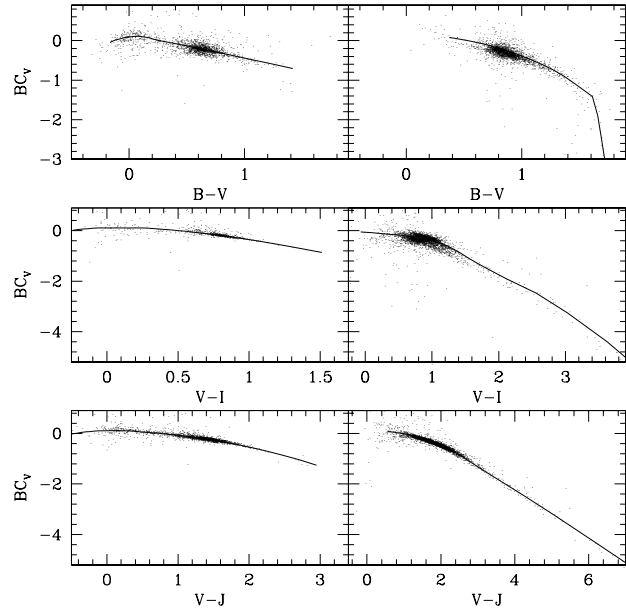


Figure 4. BC_V vs $(B-V)$, $(V-I)$ and $(V-J)$ colors for metal poor (left panels) and metal rich (right panels) stars. Continuous lines are our best fits.

3.1.2 Other bolometric corrections

Using our database we also inferred an estimate of BC_V as a function of the $(B-V)$, $(V-I)$ and $(V-J)$ colors, respectively, for metal poor and metal rich stars, as in the case of the BC_K . In Fig.4, we plot the results and in Table 3 we listed the values for the corresponding BC_K .

The possible small dependence of the $(V-K)$ color on metallicity should imply a similar dependence of the BC_V ; hence, BC_K could be a *purer* thermometer than BC_V .

Moreover, in the BC_V *vs* $(B-V)$ plane the difference between metal poor and metal rich stars is more pronounced (up to about 0.2 mag), since metallicity effects are more important at shorter wavelengths.

3.2 The determination of T_{eff}

Our photometric database does not allow us to calibrate directly an empirical temperature scale since we do not know the angular diameter of the observed stars. However DB93 provided a sample of field giants with measured angular diameters by means of Michelson interferometry and lunar occultations. We used his database, our BC scale and zero point to calibrate a new empirical relation which links the effective temperature to the BC_K .

We also provided fully theoretical temperature scales as a function of suitable colors and BC, using the grids of stellar atmospheres computed by BCP97 at solar metallicity.

3.2.1 Empirical T_{eff}

We used the DB93's giants listed in his Table 1 and 3 of DB93, for which accurate estimates of the angular diameter exist, and by means of a second order polynomial fit we obtained V fluxes as a function of the $(V-K)$ color, using our

Table 3. BC_K as a function of $(V-K)$, $(J-K)$, BC_V , $(B-V)$, $(V-I)$, $(V-J)$ colors for metal poor and metal rich stars, respectively, and both empirical and theoretical T_{eff} .

BC_K	$V-K$	$J-K$	BC_V	$B-V$	$V-I$	$V-J$	$V-K$	$J-K$	BC_V	$B-V$	$V-I$	$V-J$	T_{eff} Emp	T_{eff} Theor
Poor							Rich							
-0.40	-0.413	-0.137	0.013	-0.118	-0.241	-0.420	—	—	—	—	—	—	—	10462
-0.30	-0.338	-0.119	0.038	-0.089	-0.204	-0.360	—	—	—	—	—	—	—	10139
-0.20	-0.259	-0.099	0.059	-0.062	-0.169	-0.300	—	—	—	—	—	—	—	9824
-0.10	-0.177	-0.075	0.077	-0.040	-0.132	-0.237	—	—	—	—	—	—	—	9518
0.00	-0.091	-0.052	0.091	-0.009	-0.098	-0.176	—	—	—	—	—	—	—	9219
0.10	-0.001	-0.030	0.101	0.033	-0.068	-0.120	—	—	—	—	—	—	—	8928
0.20	0.092	-0.003	0.108	0.068	-0.032	-0.064	—	—	—	—	—	—	—	8645
0.30	0.190	0.026	0.110	0.078	-0.004	0.157	—	—	—	—	—	—	—	8370
0.40	0.292	0.055	0.108	0.078	0.203	0.234	—	—	—	—	—	—	—	8102
0.50	0.399	0.082	0.101	0.100	0.253	0.319	0.425	0.082	0.075	—	—	—	7602	7842
0.60	0.510	0.113	0.090	0.133	0.293	0.365	0.522	0.107	0.078	—	—	—	7386	7589
0.70	0.626	0.145	0.074	0.168	0.341	0.436	0.621	0.132	0.079	0.373	—	0.563	7173	7343
0.80	0.745	0.178	0.055	0.191	0.390	0.522	0.723	0.159	0.077	0.378	—	0.575	6963	7105
0.90	0.869	0.210	0.031	0.218	0.444	0.615	0.829	0.187	0.071	0.393	—	0.611	6756	6871
1.00	0.996	0.244	0.004	0.259	0.498	0.721	0.938	0.216	0.062	0.413	—	0.662	6553	6642
1.10	1.123	0.279	-0.023	0.307	0.548	0.828	1.050	0.245	0.050	0.440	—	0.724	6353	6421
1.20	1.249	0.316	-0.049	0.353	0.592	0.918	1.168	0.274	0.032	0.476	—	0.808	6156	6208
1.30	1.380	0.350	-0.080	0.406	0.642	1.018	1.289	0.305	0.011	0.516	—	0.897	5963	6003
1.40	1.506	0.385	-0.106	0.451	0.681	1.095	1.417	0.336	-0.017	0.564	—	1.003	5774	5806
1.50	1.641	0.423	-0.141	0.510	0.731	1.193	1.549	0.369	-0.049	0.614	-0.067	1.111	5589	5618
1.60	1.778	0.461	-0.178	0.572	0.782	1.289	1.688	0.405	-0.088	0.670	0.111	1.228	5407	5438
1.70	1.925	0.498	-0.225	0.651	0.843	1.402	1.834	0.444	-0.134	0.731	0.321	1.352	5229	5264
1.80	2.083	0.532	-0.283	0.747	0.915	1.531	1.987	0.486	-0.187	0.795	0.561	1.480	5056	5097
1.90	2.239	0.572	-0.339	0.838	0.981	1.647	2.147	0.533	-0.247	0.863	0.761	1.610	4887	4933
2.00	2.415	0.612	-0.415	0.961	1.066	1.792	2.317	0.582	-0.317	0.932	0.900	1.746	4723	4774
2.10	2.595	0.653	-0.495	1.088	1.152	1.934	2.498	0.634	-0.398	1.005	1.027	1.889	4563	4618
2.20	2.791	0.690	-0.591	1.239	1.250	2.090	2.691	0.689	-0.491	1.087	1.133	2.038	4406	4468
2.30	3.006	0.738	-0.706	1.416	1.362	2.263	2.900	0.747	-0.600	1.173	1.226	2.195	4254	4321
2.40	3.265	0.790	-0.865	—	1.512	2.481	3.127	0.807	-0.727	1.263	1.319	2.359	4106	4179
2.50	3.551	0.846	-1.051	—	—	2.713	3.390	0.870	-0.890	1.362	1.426	2.544	3962	4040
2.60	3.860	—	-1.260	—	—	2.950	3.703	0.937	-1.103	1.468	1.559	2.767	3819	3904
2.70	4.216	—	-1.516	—	—	—	4.117	1.006	-1.417	1.612	1.762	3.102	3667	3771
2.80	4.626	—	-1.826	—	—	—	4.696	1.077	-1.896	1.659	2.111	3.637	3523	3639
2.90	—	—	—	—	—	—	5.378	1.152	-2.478	1.690	2.564	4.268	3409	3516
3.00	—	—	—	—	—	—	6.263	1.229	-3.263	1.732	3.033	5.099	3317	3385
3.10	—	—	—	—	—	—	7.485	1.310	-4.385	1.793	3.620	6.258	3247	3243
3.20	—	—	—	—	—	—	9.444	1.393	-6.244	—	4.443	8.142	3199	2929
3.30	—	—	—	—	—	—	19.746	1.478	-16.446	—	8.119	18.471	3174	2499

zero points. We did not use DB93's linear relations since they have a discontinuity around $(V-K)=3.7$ which propagates into the relation which gives T_{eff} as a function of $(V-K)$ and BC_K .

Following the procedure described in DB93 we derived the relation:

$$\log T_{eff} = 3.9619 - 0.0466(V-K) + 0.0038(V-K)^2 - 0.1BC_K$$

Since DB93's database is at solar metallicity the previous relation can be regarded as reliable only for metal rich stars. Hence we computed the effective temperature using the latter relation only for the metal rich stars in our database and the results are reported in Fig.5 as a function of BC_K , while the mean relation is listed in Table 3. The average dispersion around the fiducial line is ~ 30 K. Outside the $1 < BC_K < 3.1$ range the relation was extrapolated.

3.2.2 Theoretical T_{eff}

The calibration of the effective temperature was performed using the grid of stellar atmospheres by BCP97 at solar metallicity. In order to evaluate the possible shift with vary-

ing metallicity we also used a grid of color indices for solar and 1/100 solar metallicity computed by Castelli (1997). These grids are based on the ATLAS9 model atmospheres in which the modification of the "approximate overshooting" to the mixing-length treatment of the convection was dropped. The indices slightly differ from the BCP97 indices owing to different passbands and zero points. For a given temperature and metallicity we interpolated the grids in gravity by means of the Vandenberg (1996) isochrones. For each star in our database we derived a mean temperature using both the $(V-K)$, $(V-J)$, $(J-K)$ colors and the BC_K .

The relations were derived in the Bessell (1990) photometric system, as adopted by BCP97 to compute their stellar atmosphere grids. On the other hand, our observed database refers to the ESO photometric system. We used the relations quoted by Bessell & Brett (1988) to transform the $(V-K)$, $(V-J)$ and $(J-K)$ colors of the models from the Bessell system to the ESO one. Moreover, since between the BC_K computed with our procedure and those of the models a systematic shift in the zero point of 0.01 mag was found (see Sect.3.1.1 and Fig.2), we added this shift to the BC_K of

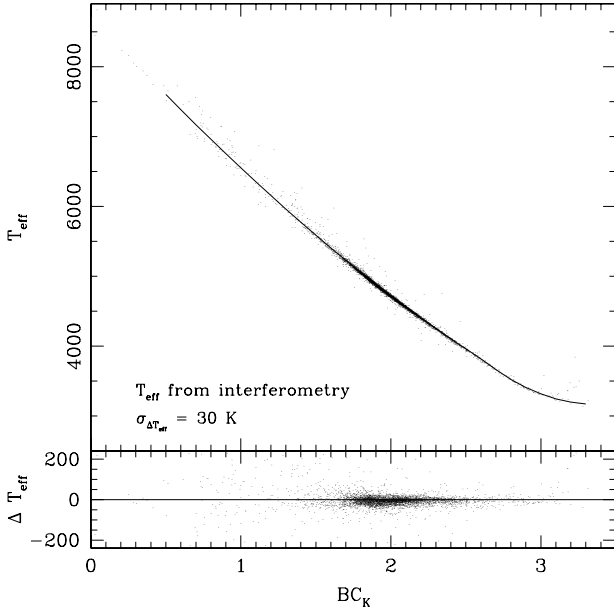


Figure 5. Empirical T_{eff} as a function of BC_K (upper panel) for metal rich stars. The continuous line is our best fit. The dispersion (on average 30 K) around the fiducial line is also plotted (lower panel).

the models. This avoids to have a systematic drift between T_{eff} derived from the colors and the BC_K .

In Fig.6 we plot the behaviour of the effective temperature as a function of both the (V-K), (V-J) and (J-K) colors in the ESO photometric system and the BC_K . Our best fits (continuous lines) are plotted as well. The spread visible in the T_{eff} vs color distributions at the lowest temperature is due to a gravity effect. It demonstrates how small variations of such a parameter may strongly affect the accuracy of the derived temperatures below 3500 K. This effect is less pronounced in the T_{eff} vs BC_K distribution. The latter is also the most linear and sensitive relation, particularly at low temperatures, confirming that BC_K is probably the *purest stellar thermometer* for cool stars.

In Fig.7 the theoretical T_{eff} derived from averaging the temperatures obtained by the color and BC_K as a function of the latter are plotted together with the dispersion (on average 180 K) around the fiducial line and in Table 3 we listed the values.

3.2.3 Comparison between the two scales

Comparing the empirical and theoretical temperature scales discussed in the previous sections, we infer the following behaviours:

- in the range 4000 – 7500 K, a general good agreement has been found, the theoretical scale being systematically warmer by about 50 K;
- between 3200 and 4000 K, this difference increases up to about 100 K;
- below 3200 K, the two scales diverge, the theoretical one becoming progressively cooler, up to 800 K.

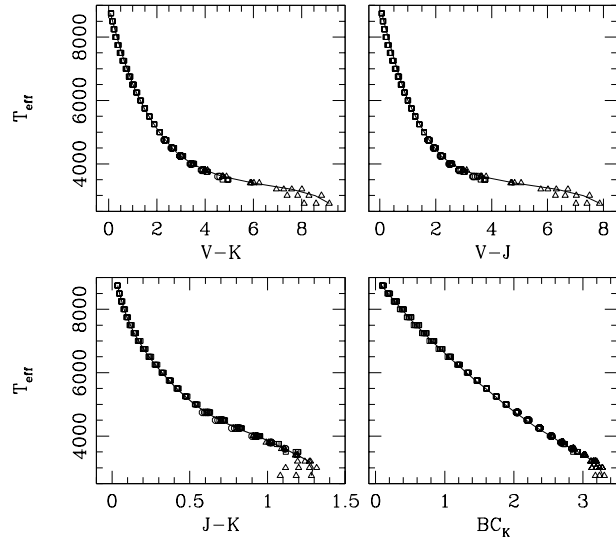


Figure 6. Theoretical T_{eff} as a function of (V-K), (V-J), (J-K) and BC_K .

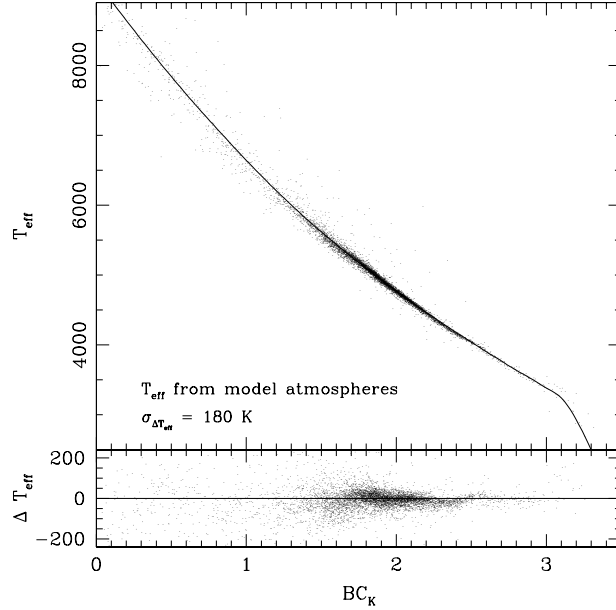


Figure 7. Theoretical T_{eff} derived from averaging the temperatures obtained by the color and BC_K as a function of the latter (upper panel). The continuous line is our best fit. The dispersion (on average 180 K) around the fiducial line is also plotted (lower panel).

The behaviour in the coolest temperature range can be explained as a gravity effect, as already mentioned in Sect.3.2.2, in the sense that the interpolation in gravity may be quite uncertain.

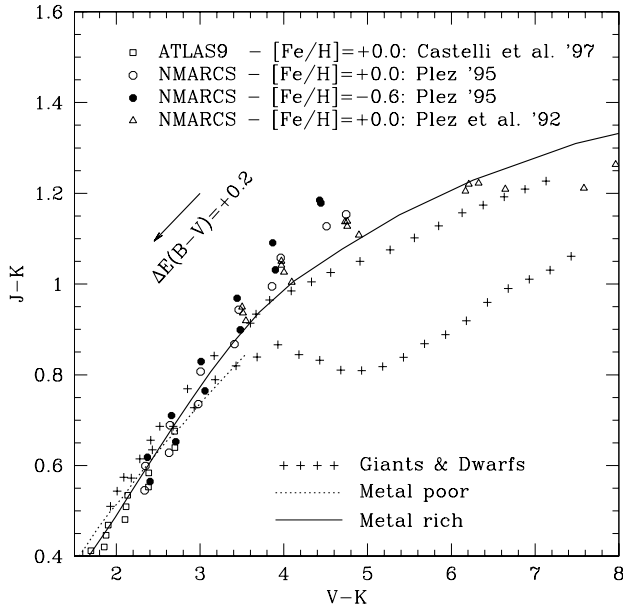


Figure 8. $(J-K)$ vs $(V-K)$ color – color diagram for the mean loci of the metal rich (continuous line) and metal poor (dashed line) observed stars and different model atmospheres. ATLAS9 models by Castelli et al. (1997) are without overshooting. The mean sequences of a sample of field giants and dwarfs by Bessell & Brett (1988) and the reddening vector are plotted as well.

4 DISCUSSION

4.1 A few more tests

In order to check the consistency between our observed database and the adopted model atmospheres, both used in the calibrations of the temperature scale (see Sect.3.2.2), we constructed a $(J-K)$ vs $(V-K)$ color – color diagram in the ESO photometric standard system for all the stars in our database (see Fig.8). The mean loci of the observed metal poor and metal rich stars, different models, and the mean sequences of a sample of field giants and dwarfs as reported in Table 2 and 3 of Bessell & Brett (1988) are plotted as well. The observed and synthetic distributions well overlap one to each other and also overlap the field giant sequence, indicating that the two photometric samples are fully consistent.

Another interesting test we performed is to apply our BC_K and T_{eff} relations to the widely used isochrones computed by Bergbusch & VandenBerg (1992), the only ones presently published in the IR–planes. Bell (1992, and reference therein) has shown how these theoretical isochrones transformed into the observational plane using the Bell & Gustafsson (1989, hereafter BG89) model atmospheres hardly reproduce the sequence of cool stars observed by Glass (1974a,b), being the former too red by ≈ 0.1 mag along the RGB.

The results of our test are plotted in Fig.9: the sequences obtained using our new calibrations well overlap those computed by using BG89 and corrected as suggested by Bell (1992) along the RGB (continuous lines), while they overlap the uncorrected ones in the turn-off region (dashed lines). Hence, it is clear that the discrepancy found

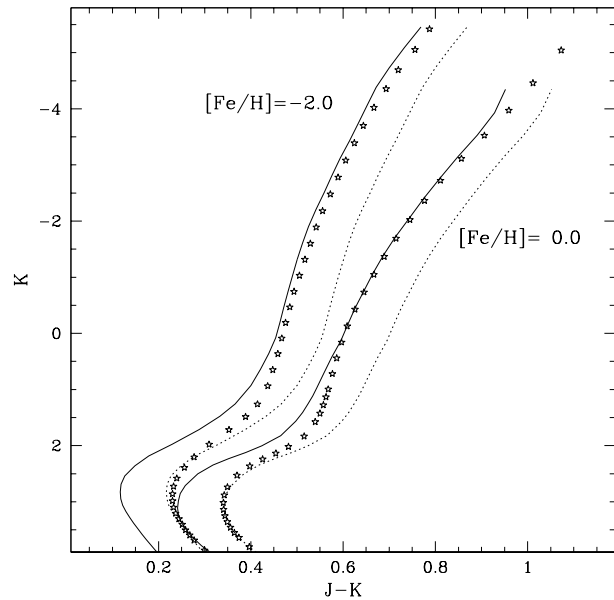


Figure 9. K vs $(J-K)$ diagram of the isochrones by Bergbusch & VandenBerg (1992) transformed into the observational plane at two different metallicities: *dotted lines* are the relations inferred using BG89 transformations, *continuous lines* represent those corrected as suggested by Bell (1992) to reproduce the observed RGB distribution, and *stars* are those obtained using our BC_K and T_{eff} transformations.

by Bell (1992) along the RGB was not due to the theoretical isochrones but should rather be a consequence of the adopted transformations into the IR observational plane.

4.2 Comparison with published BC scales

Our BCs, as reported in Table 3, in both the metal poor and metal rich regimes, were then compared with published scales.

In the BC_K vs $(V-K)$ plane, we considered the relations presented by Johnson (1966), Lee (1970), Ridgway et al. (1980), DBR87 and BG89, as tabulated by DB93 and scaled by 0.01 mag to take into account the different BC_{\odot} adopted. Moreover, we considered those obtained by FPC81, Bessell & Wood (1984), Blackwell & Petford (1991) and Alonso et al. (1995). And, finally, the BC_K of the model (BCP97), as computed to derive T_{eff} (see Sect.3.2.2), were also included.

The residuals (our – others) vs the $(V-K)$ color are plotted in Fig.10 for metal rich (lower panel) and metal poor (upper panel) stars. As can be seen, all the scales agree one to each other within 0.1 mag. Interesting enough is the opposite behaviour of ΔBC_K for metal rich and metal poor stars. While our BC_K are systematically larger than the other scales in metal rich stars, they are systematically lower in metal poor ones for a given $(V-K)$. This may reflect the fact that all the other scales average the information of the two metallicity regimes.

Concerning BC_K as a function of $(J-K)$, we compared our scale with those presented by Frogel, Persson & Cohen (1980), Bessell & Wood (1984), Bessell (1991) and with the BC_K of the model (BCP97).

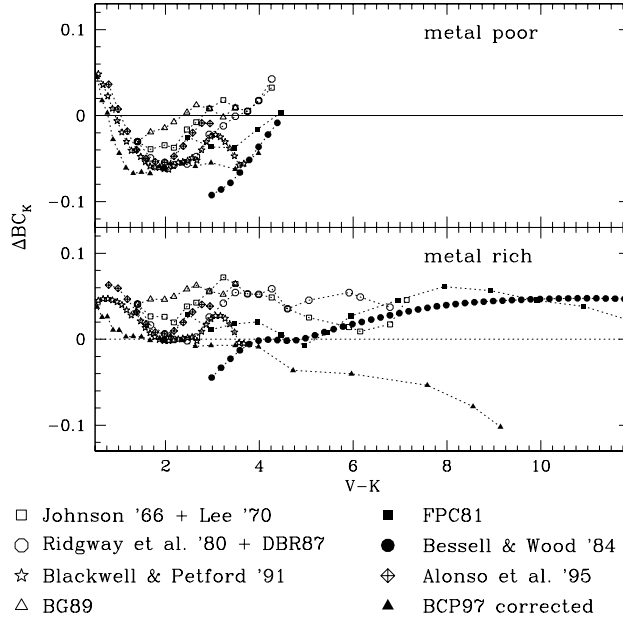


Figure 10. Comparison between our BC_K vs $(V-K)$ scale as reported in Table 3 and those obtained by other authors for metal rich (lower panel) and metal poor (upper panel) stars (see keys in the plot and Sect.4.2).

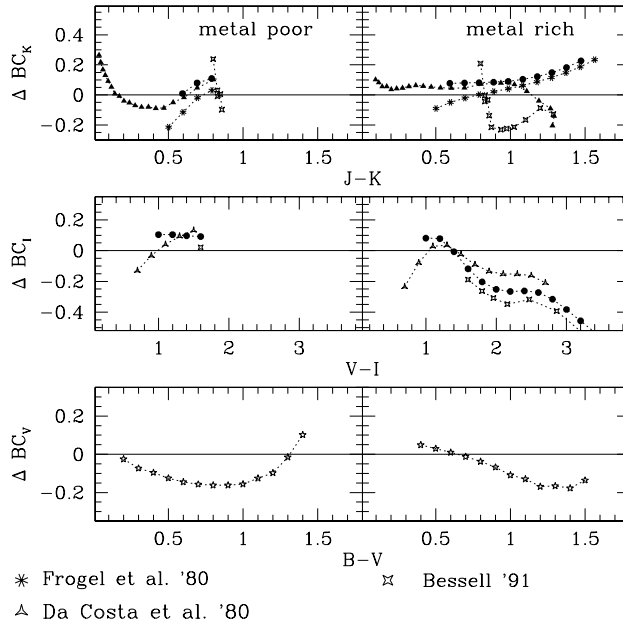


Figure 11. Comparison between our BC_K vs $(J-K)$, BC_I vs $(V-I)$ and BC_V vs $(B-V)$ scales and those by other authors for metal poor (left panels) and metal rich (right panels) stars. Keys are as in Fig.9, otherwise indicated.

The relation in the BC_I vs $(V-I)$ plane was compared with those listed by Bessell & Wood (1984), Da Costa & Armandroff (1990) and Bessell (1991).

Finally, the BC_V vs $(B-V)$ relation was compared with that obtained by Blackwell & Petford (1991).

The residuals drawn from each individual comparison vs

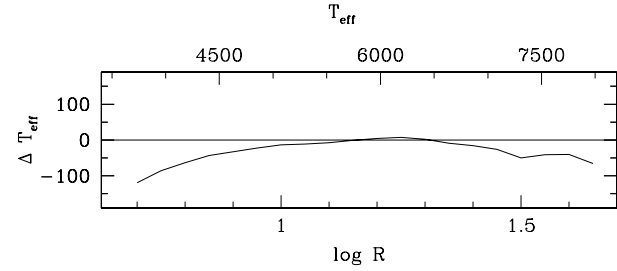


Figure 12. ΔT_{eff} vs $\log R$ and empirical T_{eff} between our empirical scales and the theoretical ones by Blackwell & Lynas-Gray (1994).

Table 4. R-parameter of the IRFM as a function of T_{eff} and BC_K .

T_{eff}	BC_K	$\log R^\dagger$	T_{eff}	BC_K	i	$\log R^\dagger$
3250	3.10	0.5504	5750	1.41	1.2235	
3500	2.82	0.6613	6000	1.28	1.2764	
3750	2.65	0.7303	6250	1.15	1.3278	
4000	2.47	0.7993	6500	1.03	1.3781	
4250	2.30	0.8676	6750	0.90	1.4275	
4500	2.14	0.9327	7000	0.78	1.4757	
4750	1.98	0.9953	7250	0.66	1.5232	
5000	1.83	1.0555	7500	0.55	1.5698	
5250	1.69	1.1134	7750	0.43	1.6158	
5500	1.55	1.1692				

† logarithmic value of $R = \frac{F_{bol}}{F_{2.2\mu m}}$ in units of μm .

the adopted colors are plotted in Fig.11 for both metal poor (left panels) and metal rich (right panels) stars. The average spread among different scales is larger in these planes than that inferred in the BC_K vs $(V-K)$ plane.

4.3 The IRFM

Using our BC_K and empirical T_{eff} we can also provide an independent, empirical calibration of the R parameter. This parameter was computed using the same ZP of our bolometric scale and the K band flux calibration of Table 2 (columns #6 and #7). The results are listed in Table 4.

This empirical scale has been compared with the relation obtained interpolating the theoretical Blackwell & Lynas-Gray (1994) grid, which tabulated $\log R$ as a function of T_{eff} and $\log g$. The interpolation in gravity was performed using the VandenBerg (1996) isochrones

In Fig.12 we plot the residual T_{eff} between the two relations as a function of our empirical $\log R$ and T_{eff} . For $\log R > 1$ there is a good agreement ($\Delta T_{eff} < \pm 50$ K) among the two relations. For $\log R < 1$ the empirical T_{eff} seem to be systematically hotter than those of the Blackwell & Lynas-Gray (1994) models.

5 CONCLUSIONS

The main results obtained from our analysis can be summarized as follow:

- By exploiting the use of a large photometric database

of Pop II stars in GGCs we derived new relations for: BC_K vs (V-K) and (J-K), BC_V vs (B-V), (V-I) and (V-J), to infer empirical bolometric corrections from observed colors.

- By making use of both an empirical relation and model atmospheres we calibrated two different scales to infer reliable stellar effective temperatures in the range 3000 – 7500 K.

- We also calibrated an empirical relation between the R parameter of the IRFM and the stellar temperature.

All these relations are summarized in Table 3, where for a given BC_K the corresponding colors and BC_V in two different metallicity regimes and T_{eff} can be read. These relations should be the most suitable to calibrate the red stellar sequences in the color–magnitude diagrams, like the RGB and AGB in old GGCs.

ACKNOWLEDGMENTS

We wish to thank all the people who kindly made available to us photometric data, model atmospheres, and isochrones. We warmly thank Mike Bessell for his very careful reading of the paper, Fiorella Castelli, Giampaolo Di Benedetto, Maria Lucia Malagnini and Bob Kurucz for helpful discussions. A special thank to the ADC Service to provide the Morel & Magnenat (1978) Catalogue. Paolo Montegriffo was supported by a 1996-grant of the *Fondazione del Monte, Rolo Banca 1473*. For their financial support, we also thank the *Ministero della Università e della Ricerca Tecnologica* (MURST) and the *Agenzia Spaziale Italiana* (ASI).

REFERENCES

Armandroff T.E., 1989, AJ 97, 375
 Auriere M., Lauzeral C., 1996, Private Communication
 Alonso A., Arribas S., Martinez–Roger C., 1995, A&A 297, 197
 Bell R.A., Gustafsson B., 1989, MNRAS 236, 653 (BG89)
 Bell R.A., 1992, MNRAS 257, 423
 Bergbusch P.A., 1996, AJ 112, 1061
 Bergbusch P.A., VandenBerg D.A., 1992, ApJS 81, 163
 Bessell M.S., 1990, PASP 102, 1181
 Bessell M.S., 1991, AJ 101, 662
 Bessell M.S., Brett J.M., 1988, PASP 100, 1134
 Bessell M.S., Castelli F., Plez B., 1997, in preparation (BCP97)
 Bessell M.S., Wood P.R., 1984, PASP 96, 247
 Blackwell D.E., Shallis M.J., Selby M.J., 1979, MNRAS 188, 847
 Blackwell D.E., Petford A.D., 1991, A&A 250, 459
 Blackwell D.E., Lynas–Gray A.E., 1994, A&A 282, 899
 Buzzoni A., 1989, AJS 71, 817
 Buzzoni A., 1996, Private Communication
 Carney B.W., Aaronson M., 1979, AJ 84, 867
 Castelli F., Gratton R.G., Kurucz R.L., 1997, A&A 318, 841
 Castelli F., 1997, Private Communication
 Da Costa G.S., Armandroff T.E., 1990, AJ 100, 162
 Di Benedetto G.P., 1993, A&A 270, 315
 Di Benedetto G.P., Rabbia Y., 1987, A&A 188, 114 (DBR87)
 Ferraro F.R., Clementini G., Fusi Pecci F., Buonanno R., 1991, MNRAS 252, 357
 Ferraro F.R., Fusi Pecci F., Guarnieri M.D., Moneti A., Origlia L., Testa V., 1994a, MNRAS 266, 829
 Ferraro F.R., Fusi Pecci F., Guarnieri M.D., Moneti A., Origlia L., Testa V., Ortolani S., 1994b, in McLean I.S., ed., Infrared Astronomy with Arrays: The next Generation. Kluwer, Dordrecht, p.235
 Frogel J.A., Persson S.E., Cohen J.G., 1980, ApJ 239, 495
 Frogel J.A., Persson S.E., Cohen J.G., 1981, ApJ 246, 842 (FPC81)
 Glass I.S., 1974a, MNRAS South Afr. 33, 54
 Glass I.S., 1974b, MNRAS South Afr. 33, 71
 Guarnieri M.D., Ortolani S., Renzini A., Montegriffo P., Moneti A., Barbuy B., Bica E., 1997, A&A (in press)
 Johnson H.L., 1966, ARAA 4, 193
 Kurucz R.L., 1979, ApJS 40, 1
 Kurucz R.L., 1993, ATLAS9 Stellar Atmosphere Programs and 2 km s⁻¹ grid, Kurucz CD-ROM No 18
 Lee S.W., 1977, A&AS 27, 367
 Megessier C., 1995, A&A 296, 771
 Montegriffo P., Ferraro F.R., Fusi Pecci F., Origlia L., 1995, MNRAS 276, 739
 Moorwood A.F.M et al., 1992, The Messenger 69, 61
 Morel M., Magnenat P. 1978, A&AS 34, 477
 Ortolani S., Desidera S., 1996, Private Communication
 Ortolani S. et al., 1995, Nature 377, 701
 Piotto G., 1996, Private Communication
 Plez B., Brett J.M., Nordlund A., 1992, A&A 256, 551
 Plez B., 1995, Private Communication
 Ridgway S.T., Wells D.C., Joyce R.R., Allen R.G., 1979, AJ 84, 247
 Rieke G.H., Lebovsky M.J., 1985, ApJ 288, 618
 Stetson P.B., 1994 PASP 106, 250
 Tinney C.G., Mould J.R., Reid I.N., 1993, AJ 105, 1045
 VandenBerg D.A., 1996, Private Communication
 Walker A.R., 1994, AJ 108, 555
 Zinn R.J., 1985, ApJ 293, 424